ℑ

Real Time Microscopy, Kinetics, and Mechanism of Giant Fullerene Evaporation

J. Y. Huang[*]

Center for Integrated Nanotechnologies (CINT), Sandia National Laboratories, Albuquerque, New Mexico 87185, USA

Feng Ding, Kun Jiao, and Boris I. Yakobson[†]
ME & MS Department, Rice University, Houston, Texas 77005, USA
(Received 31 July 2007; published 26 October 2007)

We report *in situ* high-resolution transmission electron microscopy observing the shrinkage of *single-layer* giant fullerenes (GF). At temperatures $\sim 2000\,°C$, the GF volume reduces by greater than one 100-fold while the fullerene shell remains intact, evolving from a slightly polygonized to a nearly spherical shape with a smaller diameter. The number of carbon atoms in the GF decreases linearly with time until the small subbuckyball cage opens and rapidly disappears. Theoretical modeling indicates that carbon atoms are removed predominantly from the weakest binding energy sites, i.e., the pentagons, leading to the constant evaporation rate. The fullerene cage integrity is attributed to the collective behavior of interacting defects. These results constitute the first experimental evidence for the ''shrink-wrapping'' and ''hot-giant'' fullerene formation mechanisms.

C_{60} fullerenes were first observed using mass spectrometry [1–5], but they did not immediately convince the scientific community that the structure was a hollow sphere. The early debates motivated a series of insightful and subtle ''shrink-wrapping'' experiments designed to prove that these structures are indeed hollow cages [4,5]. To this end, C_{60} clusters were impregnated with a metal atom and were then photo-fragmented to lose some carbon mass and shrink to a size bound by the endohedral metal atom. This strongly supported the concept of hollow cage where the metal atom is initially confined loosely and then wrapped tightly, terminating further shrinkage. In these studies, mass-spectrometry measurements were not complemented by direct microscopy.

Over the next decade, direct high-resolution images of remotely similar structures and their shrinkage under radiation became available [6–9]. They were typically much larger *multiwall* onions or tubes, often filled with sizable metal particles rather than a single atom. Onion layer shrinkage was due to radiation knockout of carbon atoms and was not stopped by the encapsulated matter, but rather proceeded against the internal pressure. The kinetics are apparently dominated by the transport of metal or carbon atoms through the multilayered walls and the large mismatch stress between exterior and interior parts [6–9].

Bridging these two remarkable phenomena, we observe the shrinkage of *single-layer* giant fullerenes (GF) using *in situ* high-resolution transmission electron microscopy (HRTEM) [10]. Although fullerenes have been known for over two decades, surprisingly, their formation mechanisms are still unclear. We provide the first direct evidence to the proposed ''shrink-wrap'' [4,5] mechanism and its generalization and to a recent ''hot-giant'' [11–13] mechanism. ''Shrink wrap'' refers to the creation of subsequently smaller fullerenes by removal of carbon atoms from a GF, while ''hot giant'' refers to the concept that all fullerenes

first form as GFs that are then reduced via shrink wrapping to sizes as small as a C_{60} molecule. This work also suggests a possible route to tailor the structure of fullerenes to desired sizes for device applications, or even energy storage medium [14].

Experiments are conducted in a JEOL 2010F HRTEM equipped with a Nanofactory TEM-scanning tunneling microscopy (TEM-STM) platform. The procedure is described elsewhere [15–17]. Briefly, we begin with individual multiwall carbon nanotubes (MWCNTs) that are attached on one end to a 250 μm gold rod and connected on the other end to a freshly etched gold STM probe. The MWCNT is then subjected to electric breakdown by passing through it a very high current [15], after which GFs are frequently observed inside the cavity (Fig. 1) or on the MWCNT outer surfaces (see Fig. S1 in Ref. [18]). Although the formation mechanism details are beyond the scope of this study, apparently the GFs emerge due to either shrinkage of the innermost tube layer or by curling and folding of the disrupted nanotube surface layers. These GFs are then held at high temperature to observe structural changes with time.

From previous experiments, we learned that the MWCNTs are Joule heated to temperatures $> 2000\,°C$ at high bias voltages [15–17]. At such high temperatures and in high vacuum ($< 10^{-5}$ Pa), we find that GFs shrink continuously until they reach subcritical dimensions for fullerenes, due to the systematic evaporation of carbon atoms, eventually disintegrating.

Figure 1 shows consecutive HRTEM images of the shrinkage of a GF (see also supporting movie Ml [18]). Initially two GFs [Fig. 1(a), $\sim C_{1100}$ and C_{1300} for the upper and lower ones, respectively] are present in the cavity of the MWCNT, attached side by side in a pattern we dub ''Tomanek's spectacles'', with both loops noticeably angular. The larger C_{1300} adapts the shape of the cap corner of
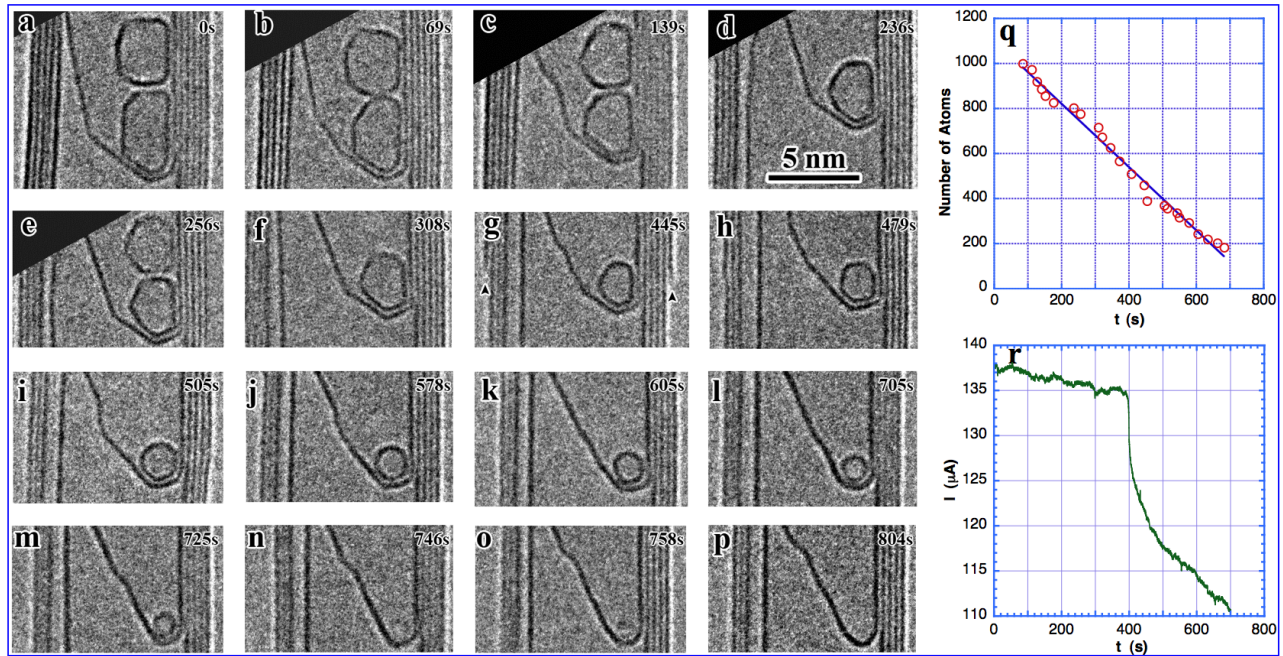
175503-1

FIG. 1 (color online). (a)–(p) Continuous shrinkage of a giant fullerene (C_{1300}) trapped inside the cavity of a MWCNT at high temperatures. The time elapse (in seconds) are marked in the figure. Note the outer diameter of the MWCNT is reduced from 9.6 nm in (a) to 9.2 nm in (p) due to evaporation of carbon atoms. (q) The number of carbon atoms in the fullerenes decrease linearly with time during the sublimation process; (r) the bias voltage in the MWCNT remains constant at 2.26 V and the current is reduced from 137 μA to 110 μA during the fullerene shrinkage process. Note that there is a sharp current drop of about 10 μA at $t = 400$ s, which is caused by the breakdown of the outmost shell [marked by two upper-pointed arrowheads in (g)]. The slow current drop is caused by the diameter reduction and defects in the MWCNT.

the inner tube wall and apparently remains trapped by van der Waals forces. The smaller C_{1100} is attached intimately to its neighbor fullerene and the innermost tube sidewall, with visibly less contact. Such weak anchoring allows the smaller GF to slide in and out of contact with the larger GF, e.g., in Fig. 1(d), this fullerene has moved out of the field of view, but in Fig. 1(e), it returns to touch the anchored piece at the same location and orientation as before (suggesting a sliding rather than rolling or a free-leap movement). After Fig. 1(f), this fullerene fragment never returns to its original position. The reason for such movement is unclear; it could be due to a static charge in the GFs, or the thermal energy, kT, sufficient to break the small van der Waals contact. Both fullerenes continuously change shape and reduce in size at high temperature (movie Ml [18]). The C_{1300}, observed throughout the entire experiment, continues to shrink, maintaining polyhedral shapes until $\sim C_{330}$ [Fig. 1(j)]. Between $\sim C_{330}$ and $\sim C_{60}$ [Fig. 1(n)], the fullerene remains closed and almost spherical. At a size $< C_{60}$, the cage structure appears to open. Once opened, it instantaneously and irreversibly disappears.

The kinetics of fullerene contraction are quantified by plotting the number of atoms N (estimated from its visible contour length) as a function of time, t. Figure 1(q) shows an approximately linear decrease in carbon atoms with time. The macroscopically expected flux rate is known to be proportional to surface area, meaning that for the present case, $dN/dt \sim N \sim e^{-\alpha t}$ (where dN/dt is the

sublimation rate and α is a constant); therefore, N should decrease exponentially with the time. In contrast, the data correspond to a constant sublimation rate $dN/dt \approx$ const. This behavior is explained below while discussing the underlying atomic mechanism of GF shrinkage.

Note that the current flowing in the MWCNT dropped continuously during the entire sublimation process [Fig. 1(r)], caused by the shrinkage of the MWCNT, defects, and electric breakdown [15–17]. Previous study showed that the temperature in a MWCNT remains unchanged despite the current decrease [19]. We conclude that the carbon atom evaporation of a fullerene is caused by the high temperature and is further facilitated by electron beam irradiation. It is unlikely that the current flow in the MWCNT influences the evaporation process since no current actually flows in the fullerene itself. Note, however, that confinement of the GFs within a MWCNT enables this experiment to be performed. Without such confinement, the GFs would sublimate intact from a surface at much lower temperatures. However, the size of the inner diameter of the MWCNT might influence the actual rate of carbon evaporation.

At graphite sublimation temperatures, some carbon atoms must escape the bonding from the fullerene cage. The probability of such events should be higher at sites where it costs less energy and can be assessed by calculating the energies of deleting a C atom or a C_2 dimer from a GF (Fig. 2). A generic example is a C_{320} molecule with

~1 nm distance between neighboring pentagons. The semiempirical parameterized model number 3 [20] method is used for computations.

It is energetically more favorable by ~3 eV to remove a C_2 from a pentagon ring than from the hexagonal lattice because the former only adds a pentagon-heptagon pair (5|7), while the latter creates a divacancy (5|8|5). Calculation also implies, irrespective of the removal sites, that removing a C_2 always takes less energy than that for a single C atom, in agreement with the known experimental fact that carbon fragmentation from fullerenes is in the units of C_2 [21–23].

From a thermodynamic point of view, a 3 eV energy difference causes a great difference in site probability by a factor of $e^{\Delta E/kT} \sim 10^6$ at the ~2000 °C experimental temperature. This huge energetic advantage of carbon removal from the pentagons easily overwhelms the greater population of hexagons (which can be more populous by hundreds) even in a very large cage. Therefore, most of the carbon loss should occur from the pentagons, offering an explanation of the constant, size-independent sublimation rate: since the number of pentagons remains nearly constant (12 is required by the Euler rule regardless of the cage size, with only minor transient $12+$ fluctuations), the leak into gas phase through these sites is not proportional to the total area but remains at steady rate. If all the additional defects generated during the C_2 sublimation are annealed or healed efficiently, the number of pentagons in the fullerene is indeed constant with time. Conversely, a constant mass loss rate infers (in addition to clean visible shape) high GF structural quality with a very low number of defects in the course of sublimation. We discuss below the basic processes responsible for both carbon removal and defect annealing.

In early studies, Smalley *et al.* proposed that a small fullerene (e.g., C_{60}) releases a C_2 dimer from a pair of adjacent pentagons (5|5) without creating any new defects [5]. Our recent study shows that at a nanotube surface, C_2
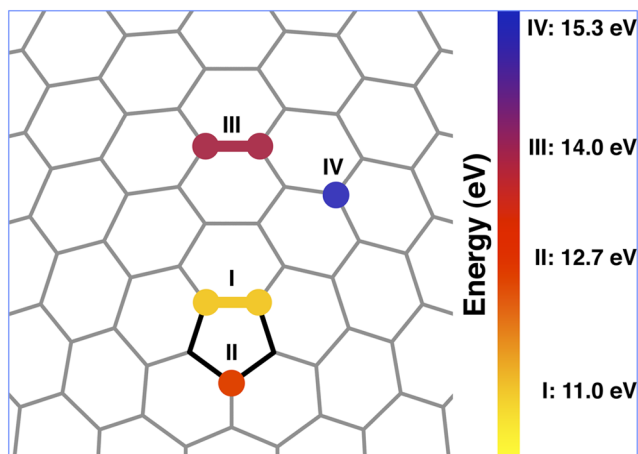
removal is facilitated by a 5|7 without creating new defects [24,25]. Here, neither adjacent (5|5) nor continuous movement of a 5|7 is possible. Figure 3(a) and 3(b) shows the defect formation after removing a C_2 from a pentagon, with a 5|7|5 topological defect created. The 5|7|5 can be viewed as a pentagon plus a 5|7 ($5 + 5|7$), which means an extra topological defect, a 5|7, was created after the C_2 removal. A 5|7 is an edge dislocation in a two-dimensional hexagonal lattice [26], and it can glide on the hexagonal lattice by rotating [Stone-Wales (SW) transformation] one of the shoulder bonds of its heptagon [24–26]. At sublimation temperatures, the 5|7 dislocation is fully activated and mobile on a GF surface. This mobility is important since the 5|7 cannot be eliminated by the parent pentagon where it was created. However, the 5|7 can easily be removed by another pentagon if it migrates over the fullerene surface. There are 11 nonparent pentagons in the fullerene, so the 5|7 can be efficiently annealed through the basic mechanisms shown in Fig. 3(c)–3(f).

Once a 5|7 encounters a pentagon, it can be annealed by a C_2 removal or by a SW bond rotation. There are two principle cases in annealing the topological defect: two adjacent pentagons with one heptagon annealed into one pentagon by removing a C_2 [Fig. 3(c) and 3(d)] or two separate pentagons and a heptagon annealed into a pentagon by a C-C bond rotation [Fig. 3(e) and 3(f)]. The above analysis shows that a pentagon can serve as either a source or a sink for topological defects (e.g., 5|7) on a fullerene surface.

A modified Monte Carlo dynamic simulation was used to track the evolution of the GF and included the carbon removal channel in the sublimation process of large fullerenes [24,25]. The initial fullerene was an icosahedral C_{720}. At each step, a C_2 was removed from the most energetically preferred sites in the fullerene after a full scan of all possible C_2 removal options. Following the C_2 removal, the most energetically favorable bond rotations were per-
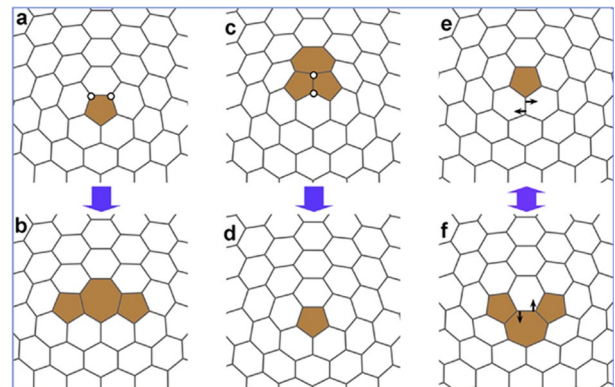

FIG. 2 (color online).   Energy cost of removing a C_2 and a C_1 from different sites in the fullerene C_{320}.

FIG. 3 (color online).   A pentagon acts as both a source and a sink of a 5|7. (a), (b) Removal of a C_2 from a pentagon creates a $5 + 5|7$ defect; (c), (d) when a 5|7 approaches to a pentagon, removal of a C_2 annihilates the 5|7 defect; (e), (f) a bond rotation step annihilates a 5|7 in the vicinity of a pentagon, and the reverse process creates an additional 5|7.
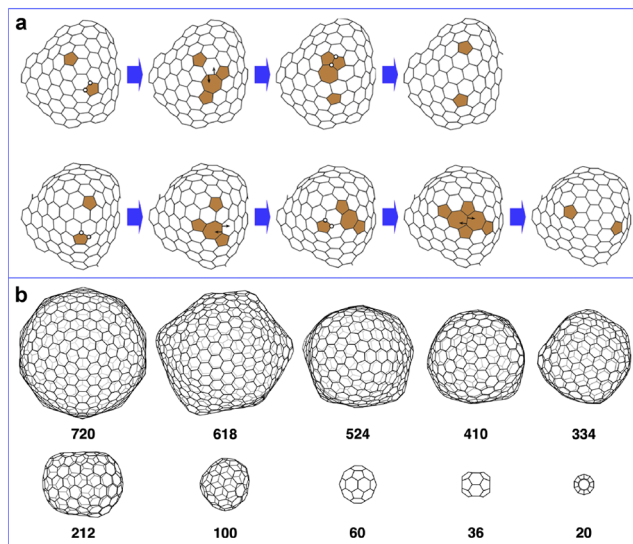
FIG. 4 (color online). Typical C_2 removal process and the annihilation of 5|7 defects in the large fullerene surface [(a), upper panel] and snapshots of the shrinking of fullerenes during the simulation process [(b), lower panel].

formed to anneal the formed topological defects until the energy could not be further reduced by any possible SW transformation. Then next C_2 was removed from the next "weakest spot", and so on. The simulation was performed with the Tersoff-Brenner interatomic potential [27].

Figure 4(a) shows a typical sequence, from a C_2 removal, followed by the formation of a 5|7 and then its annihilation, observed in the dynamic simulation. The process starts with two separated pentagons in the fullerene surface. The created 5|7 glides towards another pentagon and then is annihilated by a C_2 removal step. With this efficient annealing, a GF can avoid any hole formation and maintains its high-quality closed structure during the sublimation process. The snapshots in Fig. 4(b) clearly show that the large fullerenes undergo spherical-polyhedron shape changes, as observed in experiments. The observed GF sublimation process here agrees with recent "hot-giant" molecular dynamic simulations [11–13] and may provide the first experimental evidence of the buckyball formation mechanism, which is still unclear after more than two decades of its discovery.

In summary, giant fullerenes produced during electric breakdown and Joule heating of MWCNTs shrink continuously until they form a C_{60} molecule that then disintegrates and vanishes due to the carbon evaporation. The carbon atom evaporation rate is linear with time. Theoretical analysis indicates that carbon atoms are preferably removed from the pentagon sites and that the number of pentagons in all the GFs remains constant (twelve), consistent with the linear shrinkage rate. The shrinkage process involves both C_2 pair removal and SW (bond flip)

transformations, which together maintain the integrity of the cage structures.

*Corresponding author.
jhuang@sandia.gov
†Corresponding author.
biy@rice.edu

[1] H. W. Kroto *et al.*, Nature (London) **318**, 162 (1985).
[2] W. Kratschmer *et al.*, Nature (London) **347**, 354 (1990).
[3] H. W. Kroto and K. McKay, Nature (London) **331**, 328 (1988).
[4] S. C. O'Brien *et al.*, J. Chem. Phys. **88**, 220 (1988).
[5] R. E. Smalley, Acc. Chem. Res. **25**, 98 (1992).
[6] F. Banhart *et al.*, Chem. Phys. Lett. **269**, 349 (1997).
[7] F. Banhart and P. M. Ajayan, Nature (London) **382**, 433 (1996).
[8] D. Ugarte, Nature (London) **359**, 707 (1992).
[9] F. Banhart, Rep. Prog. Phys. **62**, 1181 (1999).
[10] H. W. Kroto, J. Chem. Soc., Faraday Trans. **86**, 2465 (1990).
[11] S. Irle *et al.*, Nano Lett. **3**, 1657 (2003).
[12] G. Zheng, S. Irle, and K. Morokuma, J. Chem. Phys. **122**, 014708 (2005).
[13] S. Irle *et al.*, J. Phys. Chem. **110**, 14 531 (2006).
[14] Y. K. Kwon, D. Tomanek, and S. Iijima, Phys. Rev. Lett. **82**, 1470 (1999); O. V. Pupysheva, A. A. Farajian, and B. I. Yakobson, Nano Lett. (to be published).
[15] J. Y. Huang *et al.*, Phys. Rev. Lett. **94**, 236802 (2005).
[16] J. Y. Huang *et al.*, Phys. Rev. Lett. **98**, 185501 (2007).
[17] J. Y. Huang, Nano Lett. **7**, 2335 (2007).
[18] See EPAPS Document No. E-PRLTAO-99-063744 for supporting material and movie. For more information on EPAPS, see http://www.aip.org/pubservs/epaps.html.
[19] X. Y. Cai, S. Akita, and Y. Nakayama, Thin Solid Films **464–465**, 364 (2004).
[20] J. P. J. Stewart, J. Comput. Chem. **10**, 209 (1989).
[21] R. F. Curl, Phil. Trans. R. Soc. A **343**, 19 (1993).
[22] J. Hunter, J. Fye, and M. F. Jarrold, Science **260**, 784 (1993).
[23] R. L. Murry *et al.*, Nature (London) **366**, 665 (1993).
[24] F. Ding *et al.*, Nano Lett. **7**, 681 (2007).
[25] F. Ding *et al.*, Phys. Rev. Lett. **98**, 075503 (2007).
[26] B. I. Yakobson, Appl. Phys. Lett. **72**, 918 (1998).
[27] D. W. Brenner, Phys. Rev. B **42**, 9458 (1990).